Digest Journal of Nanomaterials and Biostructures Vol. 6, No 4, October-December 2011, p. 1887-1895

INFLUENCE OF THE CHEMICAL STRUCTURE OF ORGANIC POLLUTANTS ON PHOTOCATALYTIC ACTIVITY OF TiO_2 NANOPARTICLES: KINETIC ANALYSIS AND EVALUATION OF ELECTRICAL ENERGY PER ORDER (E_{EO})

MOHAMMAD A. BEHNAJADY[*], HAMED ESKANDARLOO, NASSER MODIRSHAHLA, MOHAMMAD SHOKRI
Department of Chemistry, Faculty of Science, Islamic Azad University, Tabriz Branch, Tabriz, I. R. Iran

Photocatalytic degradation of different organic pollutants such as C.I. Acid Red 27(AR27), Methyl Orange (MO), Malachite Green (MG) and 4–Nitrophenol (4–NP) were investigated under UV light irradiation using synthesized TiO_2 nanoparticles by sol–gel method. It was found that the photocatalytic degradation rate depends on pollutants structure. The results indicate that from these pollutants MG can be removed faster than other pollutants. Also, 4–NP with a more stable structure than other pollutants has lowest removal rate in the presence of TiO_2 nanoparticles under UV light irradiation. The results prove that removal rate of pollutants with different structures follows pseudo–first order kinetics. The figures–of–merit based on electric energy consumption (electrical energy per order (E_{EO})) were evaluated in the photocatalytic degradation of four organic pollutants. The results indicate that E_{EO} values depend on the basic structure of the pollutants.

(Received October 7, 2011; accepted December 5, 2011)

Keywords: Photocatalytic degradation; Organic pollutants; Titanium dioxide nanoparticles; Electrical energy per order; Kinetic analysis; sol-gel

1 Introduction

Environmental pollution and destruction on a global scale, as well as the shortage of sufficient clean and natural energy sources, have attracted much attention to the vital need for developing ecologically clean and safe chemical technology, materials, and processes [1,2]. Dye molecules are extensively used in textile dyeing, paper printing, leather, pharmaceutical, cosmetic, and nutrition industries [3,4]. Textile industries generate wastewaters that contain considerable amounts of non–fixed dyes and a huge amount of inorganic salts [5,6]. The principle sources of environmental aqueous contamination in wastewaters are dye pollutants. They need to be removed from wastewaters by different methods. The most often used methods for the treatment of these textile dyes, including membrane filtration, adsorption, biological degradation (biodegradation), ozonation, are not efficient enough [7,8]. Advanced oxidation processes (AOPs) seem to be a very promising way to deal with the problem of organic pollutants destruction in aqueous systems [9]. Among the AOPs, heterogeneous photocatalysis was found as an emerging destructive technology leading to the total mineralization of most organic pollutants [10,11]. Heterogeneous photocatalysis involves combination of UV light and a semiconductor catalyst such as TiO_2 and ZnO usually in suspension mode in aqueous solution. When a semiconductor absorbs a photon with energy greater than or equal to the band gap energy produces electron–hole pairs within the conduction and valence bands (Figure 1) [12]. Generated electron–hole pairs can either recombine and release heat energy or interact separately with other molecules [13]. Organic pollutants can be degraded and ultimately mineralized completely with UV–illuminated TiO_2 powder [14]. Due to the wide band gap (3.2 eV); stimulation of TiO_2 is required using UV light. The interest in TiO_2

---

[*] Corresponding author: behnajady@gmail.com, behnajady@iaut.ac.ir

was mainly due to its availability, high stability, non–environmental impact, optical–electronic properties, low cost and considerable photocatalytic activity [15,16].

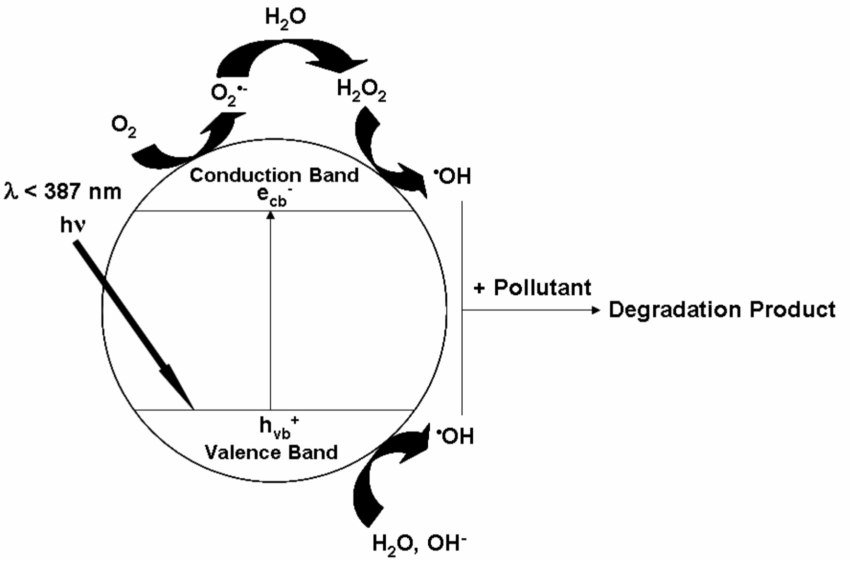

Fig. 1. Scheme of the photocatalytic process over titanium dioxide.

Recently some researchers have reported the photocatalytic degradation of C.I. Acid Red 27 (AR27), Methyl Orange (MO), Malachite Green (MG) and 4–Nitrophenol (4–NP) with TiO_2 in the presence of UV or visible light [17-26]. Other researchers have compared the photocatalytic degradation of various organic dyes to determine the influence of the chemical structure of dyes on the degradation rate. Mozia [27] has compared the photocatalytic degradation of three azo dyes, two monoazo dyes: C.I. Acid Red 18 and C.I. Acid Yellow 36, and one poly azo dye C.I. Direct Green 99 in water under UV irradiation. Hu et al. [28] have studied the photocatalytic degradation of three azo dyes in UV illuminated TiO_2 dispersions. Guillard et al. [29] have compared the photocatalytic degradation of two types of dyes (anionic and cationic dyes) by using UV–irradiated TiO_2 in suspension or supported on glass and paper. Abo–Farha [30] has compared the photocatalytic degradation of two azo dyes, (i.e. monoazo dye C.I. Acid Orange 10 and diazo dye C.I. Acid Red 114) present in wastewater with TiO_2 semiconductor under UV–visible light illumination. Wang [31] has investigated the photocatalytic degradation of eight commercial dyes with different structure and containing different substitute groups using TiO_2 as photocatalyst in aqueous solution under solar irradiation.

The aim of the present work is the comparison of photocatalytic activity of TiO_2 nanoparticles prepared with sol–gel method in the removal of four different organic pollutants with diverse chemical structure (AR27, MO, MG and 4–NP), kinetic analysis and also evaluation of electrical energy consumption. TiO_2 nanoparticles with high surface area and photocatalytic activity were prepared by sol–gel method in the presence of methanol as solvent.

2 Materials and methods

2.1 Materials

AR27, MO, MG and 4–NP, all from Merck, were four pollutant studied in these experiments without any further purification. Table 1 summarizes complete characterization of these organic pollutants.

Table 1. Summarization of organic pollutants characterization.

Organic pollutant	Chemical structure	Properties		
		Chemical formula	Molecular weight (g mol^{-1})	Absorption max (nm)
C.I. Acid Red 27 (AR27)	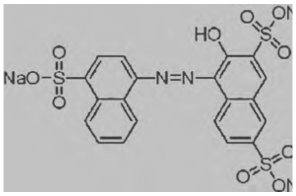	$C_{20}H_{11}N_2Na_3O_{10}S_3$	604.473	522
Methyl Orange (MO)	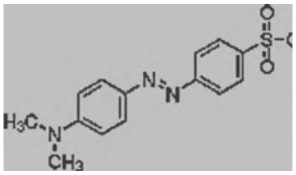	$C_{14}H_{14}N_3NaO_3S$	327.33	464
Malachite Green (MG)	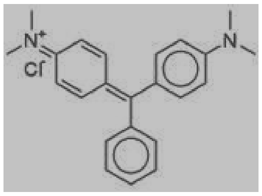	$C_{23}H_{25}ClN_2$	364.911	617
4–Nitrophenol (4–NP)	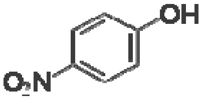	$C_6H_5NO_3$	139.11	400

In our previous work, we reported synthesis of TiO_2 nanoparticles with high surface area and high photocatalytic activity by sol–gel route [32]. Initially, titanium precursor ($Ti(OC_3H_7)_4$, TTIP) was slowly dissolved in methanol with molar ratios 1:1. Then, the obtained titanium solution was sonicated in an ultrasonic bath (Elma, T460/H, 35 kHz, 170 W). The hydrolysis process was then performed by adding of drop wise water into a flask containing (precursor/solvent) mixture under reflux and magnetic stirring for 3 h at 80°C. The molar ratio of H_2O, methanol and TTIP were 65:1:1. The obtained sol was dried at 80°C and finally calcined in air at 450°C during 3 h.

Structure, size, band gap and specific surface area of synthesized TiO_2 nanoparticles have been characterized by X–ray diffraction, transmission electron microscopy, UV–Vis reflectance spectroscopy and BET analysis. It was found that TiO_2 nanoparticles containing with crystallite size in the range of 12–15 nm. The synthesized TiO_2 exhibited specific surface area of 99.71 m^2 g^{-1}, mean pores diameter of 8.7 nm and band gap energy 3.28 eV [32]. The TEM image of the synthesized TiO_2 nanoparticles has been shown in Fig. 2.

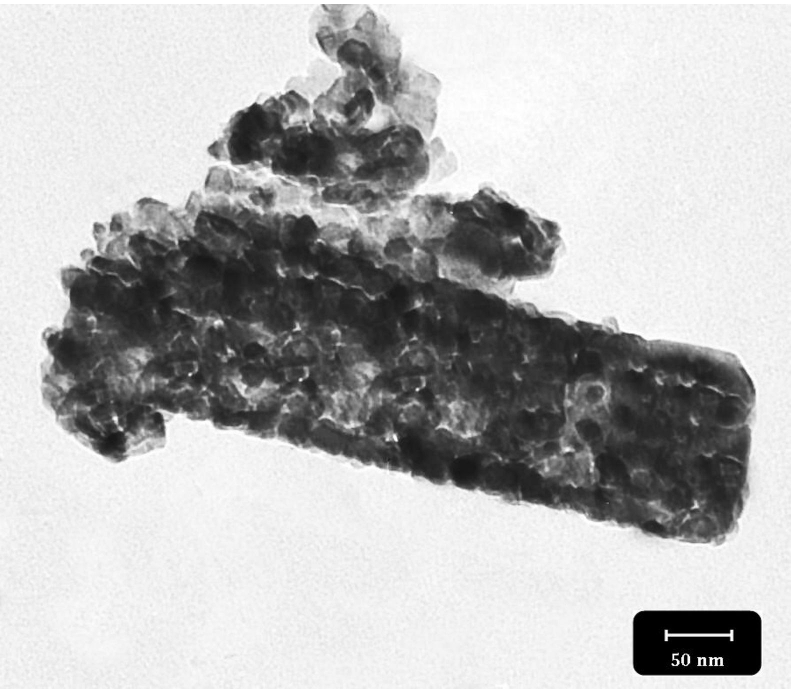

Fig. 2. TEM image of the synthesized TiO_2 nanoparticles.

2.2 Photoreactor and procedure

Photocatalytic activity measurements were carried out at room temperature in a batch quartz reactor. Artificial irradiation was provided by 15 W (UV–C) mercury lamp (Philips, Holland) emitted around 254 nm, positioned parallel to the reactor, as previously reported [33]. In each run, 40 mg of TiO_2 was dispersed in 100 mL water for 15 min using an ultrasonic bath (Elma T460/H, 35 kHz, 170 W), then desired concentration of organic pollutants ($[MG]_o = 5$ mg L^{-1}, $[AR27]_o = 20$ mg L^{-1}, $[MO]_o = 10$ mg L^{-1}, $[4\text{–}NP]_o = 20$ mg L^{-1}) and TiO_2 (400 mg L^{-1}) were fed into the quartz tube reactor. The reaction cell was bubbled with O_2 at a flow rate of 0.5 mL min^{-1} in the darkness for 30 min before irradiation. At given irradiation time intervals, the samples (5 mL) were taken out, centrifuged (Hettich EBA) and then analyzed by UV–Vis spectrophotometer (Pharmacia Biotech, Ultrospec 2000).

3 Results and discussion

3.1 Kinetics analysis

Photocatalytic degradation of organic pollutants in aqueous media considerably is in the result of producing highly reactive hydroxyl radicals. Hydroxyl radicals are short lived and non selective reagent in reaction with organic pollutants. With considering this fact we propose the following rate law for photocatalytic degradation of organic pollutants in the UV/TiO_2 process:

$$-r_C = k[^{\circ}OH]_{ads}[C]_{ads} \quad (1)$$

where k is the rate constant, $[^{\circ}OH]_{ads}$ is the adsorbed concentration of hydroxyl radicals and $[C]_{ads}$ is the adsorbed organic pollutant concentration.

It is proved that hydroxyl radicals and organic compounds are adsorbed on different sites, and adsorption of intermediate and organic compound are competitive on the same sites [34].

According to the results of Rideh et al. [35] the adsorption of these compounds are Langmuir type. With considering these findings, the reaction rate may be expressed as follows:

$$-r_C = k\left(\frac{K_{^\circ OH}[^\circ OH]}{1+K_{^\circ OH}[^\circ OH]}\right)\left(\frac{K_C[C]}{1+K_C[C]+\sum_i K_i[I_i]}\right) \quad (2)$$

In this equation $K_{^\circ OH}$, K_C and K_i are the adsorption equilibrium constant for hydroxyl radicals, organic pollutants and intermediates, respectively. Also, I_i is the concentration for intermediates.

Beltran−Heredia et al. [36] made the following change by considering this assumption in which the adsorption coefficients for all organic molecules are the same:

$$K_C[C]+\sum_i K_i[I_i] = K_C[C]_0 \quad (3)$$

where $[C]_0$ is initial concentration of organic pollutant. With considering that in all experiments of this work oxygen concentration, dosage of catalyst and light intensity were constant, therefore for all runs the fraction sites covered by hydroxyl radicals was also constant, therefore we can write following equation:

$$k' = k\left(\frac{K_{^\circ OH}[^\circ OH]}{1+K_{^\circ OH}[^\circ OH]}\right) \quad (4)$$

Finally, Equation (5) can be written as:

$$-r_C = -\frac{dC}{dt} = k'\left(\frac{K_C[C]}{1+K_C[C]_0}\right) = k_{app}[C] \quad (5)$$

in this equation k_{app} is the pseudo–first order reaction rate constant which is a function of various operational parameters. With integrating Equation (5) we obtain following equation:

$$\ln\frac{[C]_0}{[C]} = k_{app}t \quad (6)$$

The semi–logarithmic graph of the concentration of organic pollutants in the presence of TiO_2 nanoparticles prepared with sol–gel method versus irradiation time (Fig. 3.) yield straight lines, which confirm the pseudo–first order kinetics for decolorization of organic pollutants in this process. Pseudo–first order reaction rate constants (k_{app}) for different organic pollutants were obtained from the slope of these lines according to Equation (6).

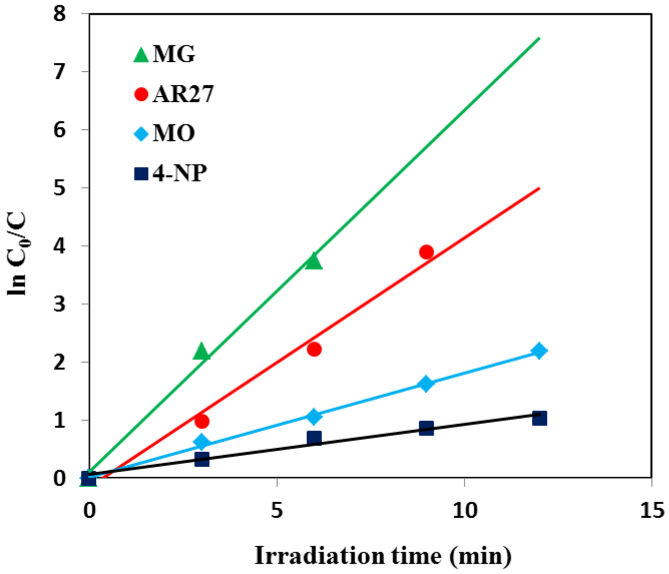

Fig. 3. The semi–logarithmic plot of different organic pollutants concentration versus UV irradiation time.

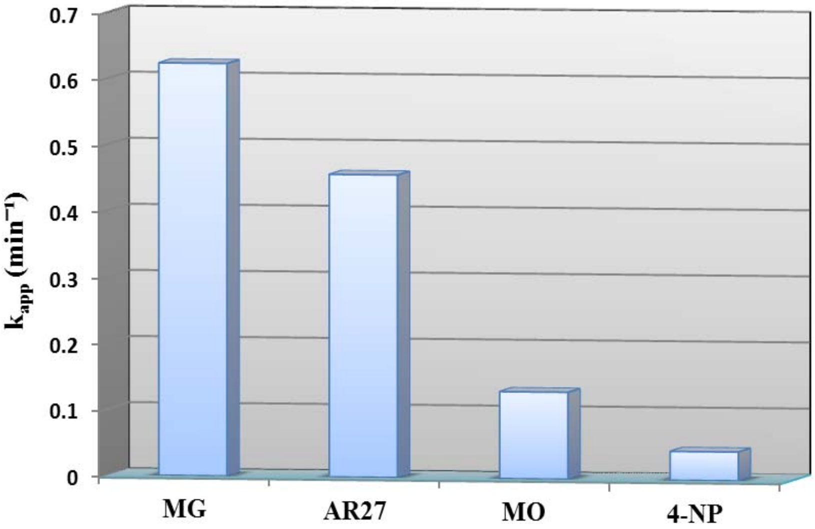

Fig. 4. Plot of k_{app} for different organic pollutants in UV/TiO_2 process.

Fig. 4. shows the variation of k_{app} for removal of MG, AR27, MO and 4–NP with UV/TiO_2 process. As can be seen, the removal rate is different for various organic pollutants so that k_{app} is the highest for MG and the lowest for 4–NP.

The k_{app} values are in the following order: MG > AR27 > MO > 4–NP, meaning that the photocatalytic activity of the TiO_2 nanoparticles varies with the nature of the substrates. The difference between the k_{app} values for these contaminants can be explained by their variation in molecular structures. The k_{app} for 4–NP is lowest, this may be attributed to the stable structure of 4–NP that making it less photodegradable. The resistance of 4–NP to photodegradtion might be associated with the presence of electron donating hydroxyl (–OH) and amino (–NO_2) groups with resonance effect in the chemical structure of 4–NP, which probably stabilizes the 4–NP molecule.

In azo–dyes, such as AR27 and MO both nitrogen atoms in the azo–groups have zero oxidation degree [29]. The smaller removal rate constant of MO in comparison with AR27 can be explained by the presence of methyl group (–CH_3) in the MO molecular structure. The presence of the methyl group in MO molecular structure can decrease the solubility of this molecule in water. Hydroxyl radicals are very reactive and have very short lifetime, so that they can only react in the location of formation. Therefore, every group that causes to decrease the solubility of molecules in water will reduce the removal rate [37].

The higher degradability of MG could be due to the presence of a positively charged N^+ group in MG molecular structure. Irradiation of TiO_2 nanoparticles with UV light at lower than 390 nm generates electron–hole pairs. The positively charged MG molecules are interacted by the excited electrons of the TiO_2 nanoparticles and this leads to the oxidation of MG through holes. AR27 and MO molecules with negatively charged sulfonic groups (–SO_3^-) repel the excited electrons of the TiO_2 nanoparticles which promotes the recombination of the electron–hole pairs leading to the termination of photocatalytic process [38].

3.2 Electrical energy determination

In UV/TiO_2 process electric energy consumption can be a major fraction of the operating costs, therefore simple figures–of–merit based on electric energy consumption can be very useful and informative. Bolton et al. [39] defined the figures–of–merit "electric energy per order" (E_{EO}) for using in the first order kinetic regime of AOPs. This concept was accepted by the IUPAC as a technical report. The E_{EO} (kWh/m^3/order) can be calculated from the following equation:

$$E_{EO} = \frac{P_{el} \times t \times 1000}{V \times 60 \times \log\left(\frac{[C]_0}{[C]}\right)} \quad (7)$$

in this equation P_{el} is the input power (kW) to AOP system, t is the irradiation time (min), V is the volume of water (L) in the reactor, $[C]_0$ and $[C]$ are the initial and final pollutant concentrations, respectively [39]. This equation for a pseudo–first order reaction in a batch reactor changes to:

$$E_{EO} = \frac{38.4 \times P_{el}}{V \times k_{app}} \quad (8)$$

in this equation k_{app} is the pseudo–first order reaction rate constant (min^{-1}).

Table 2. E_{EO}values for photodegradation of the four organic pollutants

Organic pollutants	E_{EO} (kWh m^{-3} $order^{-1}$)
MG	9.23
AR27	12.59
MO	34.80
4–NP	72.27

Electrical energy required to the removal of four different organic pollutants at the same conditions have been given in Table 2. According to this Table, less energy was consumed during the removal of MG in comparison to other pollutants. E_{EO} amount for 4–NP is 8 times more than that of MG. This is a significant consideration in view of the evaluation of the treatment costs for the industrial applications as electric energy can correspond to a major fraction of the operating costs.

4. Conclusions

This study demonstrates that heterogeneous photocatalysis is a very effective technology for degrading organic pollutants with different structures. The experimental results indicate that the photocatalytic activity of TiO_2 nanoparticles prepared by sol–gel method is highly depending on the structure of pollutants. The difference was due to the variation in chemical structure and substitute groups of organic pollutants. Kinetic analysis indicates pseudo–first order kinetic for all of organic pollutants and the photocatalytic rate constants were in the following order: MG > AR27 > MO > 4–NP. The results of electrical energy per order (E_{EO}) evaluation show that electrical energy consumption is directly proportional to organic pollutants structure, so that 4–NP with stable structure needs more electrical energy consumption in comparison to other reactive pollutants such as MG, AR27 and MO.

Acknowledgements

The authors would like to thank the Islamic Azad University – Tabriz branch and the Iranian Nanotechnology Initiative Council for financial supports.

References

[1] M. Anpo, Stud. Surf. Sci. Catal. **130**, 157 (2000).
[2] M. Anpo, S. Dohshi, M. Kitano, Y. Hu, M. Takeuchi, M. Matsuoka, Annu. Rev. Mater. Res. **35**, 1 (2005).
[3] S. Ren, J, Guo, G. Zeng, G. Sun, Appl. Microbiol. Biotechnol. **72**, 1316 (2006).
[4] I. Arslan, I.A. Balcioglu, D.W. Bahnemann, Dyes Pigm. **47**, 207 (2000).
[5] A.B. Dos Santos, F.J. Cervantes, J.B. Van Lier, Biores. Technol. **98**, 2369 (2007).
[6] R. Mass, S. Chaudhari, Process Biochem. **40**, 699 (2005).
[7] S.G. Schrank, J.N.R. Santos, D.S. Souza, E.E.S. Souza, J. Photochem. Photobiol. A **186**, 125 (2007).
[8] N. Daneshvar, M.A. Behnajady, M. Khayyat Ali Mohammadi, M.S. Seyed Dorraji, Desalination **230**, 16 (2008).
[9] S. Song, L. Xu, Z. He, H. Ying, J. Chen, X. Xiao, B. Yan, J. Hazard. Mater. **152**, 1301 (2008).
[10] N.M. Mahmoodi, M. Arami, N.Y. Limaee,N.S. Tabrizi, J. Colloid Interface Sci. **295**, 159 (2006).
[11] I.K. Konstantinou, T.A. Albanis, Appl. Catal. B **49**, 1 (2004).
[12] J.M. Herrmann, Catal. Today **53**, 115 (1999).
[13] E. Evgenidou, I. Konstantinou, K. Fytianos, I. Poulios, T. Albanis, Catal. Today **124**, 156 (2007).
[14] J. Li, C. Chen, J. Zhao, H. Zhu, J. Orthman, Appl. Catal. B **837**, 331 (2002).
[15] A. Fujishima, T.N. Rao, D.A. Truk, J. Photochem. Photobiol. C **1**, 1 (2000).
[16] S.S. Hong, M.S. Lee, C.S. Ju, G.D. Lee, S.S. Park, K.T. Lim, Catal. Today **93–95**, 871 (2004).
[17] Y. Bessekhouad, D. Robert, J.V. Weber, J. Photochem. Photobiol. A **157**, 47 (2003).

[18] C.C. Chen, C.S. Lu, Y.C. Chung, J.L. Jan, J. Hazard. Mater. **141**, 520 (2007).
[19] S. Ruan, F. Wu, T. Zhang, W. Gao, B. Xu, M. Zhao, Mater. Chem. Phys. **69**, 7 (2001).
[20] S. Al–Qaradawi, S.R. Salman, J. Photochem. Photobiol. A **148**, 161 (2002).
[21] H. Yang, K. Zhang, R. Shi, X. Li, X. Dong, Y. Yu, J. Alloys Compd. **413**, 302 (2006).
[22] N. Daneshvar, M. Rabbani, N. Modirshahla, M.A. Behnajady, J. Environ. Sci. Health A **39**, 2319 (2004).
[23] M.A. Behnajady, N. Modirshahla, N. Daneshvar, M. Rabbani, Chem. Eng. J. **127**, 167 (2007).
[24] D. Chen, A.K. Ray, Water Res. **32**, 3223 (1998).
[25] N. San, A. Hatipoglu, G. Koçtürk, Z. Çınar, J. Photochem. Photobiol. A **146**, 189 (2002).
[26] M.A. Behnajady, N. Modirshahla, Photochem. Photobiol. Sci. **5**, 1078 (2006).
[27] S. Mozia, Pol. J. Chem. Tech. **10**, 42 (2008).
[28] C. Hu, J.C. Yu, Z. Hao, P.K. Wong, Appl. Catal. B **46**, 35 (2003).
[29] C. Guillard, H. Lachheb, A. Houas, M. Ksibi, E. Elaloui, J.M. Herrmann, J. Photochem. Photobiol. A **158**, 27 (2003).
[30] S.A. Abo–Farha, J. Am. Sci. **6**, 130 (2010).
[31] Y. Wang, Water Res. **34**, 990 (2000).
[32] M.A. Behnajady, H. Eskandarloo, N. Modirshahla, M. Shokri, Desalination (2011), doi:10.1016/j.desal.2011.04.019.
[33] M.A. Behnajady, N. Modirshahla, M. Shokri, H. Elham, A. Zeininezhad, J. Environ. Sci. Health A. **43**, 460 (2008).
[34] N. Daneshvar, M. Rabbani, N. Modirshahla, M.A. Behnajady, J. Photochem. Photobiol. A **168**, 39 (2004).
[35] L. Rideh, A. Wehrer, D. Ronze, A. Zoulalian, Catal. Today **48**, 357 (1999).
[36] J. Beltran–Heredia, J. Torregrosa, J.R. Dominguez, J.A. Peres, J. Hazard. Mater. **83**, 255 (2001).
[37] A.R. Khataee, M.B. Kasiri, J. Mol. Catal. A **328**, 8 (2010).
[38] B. Esen, T.R. Yumak, A. Sınag, T. Yıldız, Photochem. Photobiol. **87**, 267 (2011).
[39] J.R. Bolton, K.G. Bircger, W. Tumas, C.A. Tolman, Pure Appl. Chem. **73**, 627 (2001).